Evaluation of Neutron Radiation Damage in Zircaloy Fuel Clad of Nuclear Power Plants: A Study Based on PKA and dpa Calculations

Omid Noori-kalkhoran[a,1] , Massimiliano Gei[a]

[a]*School of Engineering, Cardiff University, The Parade, Cardiff CF24 3AA, Wales, UK*

Emails: NoorikalkhoranO@cardiff.ac.uk, GeiM@cardiff.ac.uk

Number of manuscript pages: 26

Number of Figures: 14

Number of Tables: 6

[1] Corresponding Author. Email address: NoorikalkhoranO@Cardiff.ac.uk

Abstract

During the lifetime of nuclear power plants, irradiation and mechanical interactions can cause permanent damage to their structural materials. In nuclear reactors, one of the most important of these materials is fuel clad that, in addition to its main role in transferring heat from fuel to coolant, restrains most of the radioactive fission products within its volume. In this article, neutron-induced radiation damage based on Primary Knock-on Atom (PKA) and displacement per atom (dpa) calculations are evaluated on fuel clad in Hot Fuel Assembly (HFA) in a WWER-1000 reactor core as a case study. New couplings of existing nuclear and radiation damage codes and methods are developed for dpa calculations and results are compared together and against experimental results. In the first step, the full reactor core is simulated with MCNPX code (v2.7) to determine the HFA and its relevant neutron-energy spectrum. SPECTER, SPECTRA-PKA and PTRAC card of MCNPX are then employed to evaluate the PKA spectrum under neutron bombardment. Finally, dpa calculated with the Binary Collision Approximation approach is achieved through the use of SRIM-2013 code. A MATLAB interchange program is developed to prepare and transfer the data between the mentioned codes and SRIM. Comprehensive comparisons are performed between results in terms of dpa obtained by (i) NRT calculation (NRT-dpa) (SPECTER and SPECTRA-PKA results), (ii) arc-dpa calculation (MCNPX+arc-dpa), (iii) BCA calculation (PTRAC+SRIM) and (iv) coupled calculation (SPECTRA-PKA+SRIM) (all generations of knock-on atoms and clusters are tracked in the last two methods). These comparisons reveal the portions of damage in Zircaloy due to PKAs, secondary knock-on atoms and cascade atoms, the effect of position-depended PKA and the fraction of displaced atoms that come back to their lattice positions as a result of thermal effects and annealing. Effects of elemental PKA are obtained by means of SPECTRA-PKA code and a visualization map of radiation damage in the clad is presented as an outcome of the SRIM code simulation. Results confirm that value of dpa calculated by MCNPX+arc-dpa is closer to experimental ones as the recombination effect in radiation damage is considered in this method.

Keywords: Radiation damage; Structural material; Fuel clad; PKA; dpa

1.Introduction

One of the main consequences of the interaction of high-energy particles (photons, neutrons, ions or electrons) with materials is the formation of damage and lattice defects resulting from the transfer of energy towards the atoms. The types of damage can in most cases be divided into two categories: (i) the primary damage that is formed immediately (within a few picoseconds) after the ion/neutron/electron impact by atomic collision processes far from thermodynamic equilibrium, and (ii) the long-time scale (nanoseconds to years) damage evolution caused by thermally activated processes (Nordlund et al., 2015). The main parameter for qualitative and quantitative comparison of radiation damage is called "displacement per atom" or dpa. Displacement per atom is the number of times that an atom is displaced for a given fluence. For the comparison of the evolution of microstructural features under different sources of irradiation, the dpa per unit volume may be the most useful measure of damage (Adrych-Brunning et al., 2018). To calculate the dpa as a reference for radiation damage, the first step is to predict how the energetic particles, like neutrons, can induce Primary Knock-on Atoms (PKAs) to leave their locations in the lattice and how these will continue to make collision cascades. Different methods and codes have been developed to calculate the PKA spectrum. SPECTER (Greenwood and Smither, 1985) and SPECTRA-PKA (Gilbert et al., 2015; Sublet et al., 2017) codes combine neutron radiation spectrum with nuclear recoil data to produce the PKA spectrum. Although both codes use the same method to achieve the goal, their outcomes are slightly different as they use different data libraries. PHITS code (Iwamoto et al., 2013) implements screened Coulomb scattering to evaluate the energy of the target primary knock-on atoms created by the projectile and the secondary particles. DART code (Lunéville et al., 2006) is based on Binary Collision Approximation (BCA) method (Robinson, 1994) and calculates the number of displaced atoms by solving the integro-differential interatomic potential equations.

Nuclear power plants (NPPs) are one of the main sources of high-energy particles such as neutrons, protons, electrons and photons. Due to the high neutron flux inside the NPP's core, their structural materials are subjected to intense radiation damage that in turn may lead to modification of physical, electrical and mechanical properties of the material, putting therefore the NPP on safety risks.

Due to the importance of the quantification of radiation damage, different studies have dealt with the estimation of this quantity in NPP structural materials (e.g. steel pressure vessel and Zirconium clad). In most of these investigations, a common approach was used to reach the goal, based on the following milestones: a) PKA calculations by using available codes or by developing new *ad-hoc* algorithms; b) evaluation of dpa by means of NRT (Norgett, Torrens and Robinson) model (Norgett

et al., 1975) or BCA. Boehmer et al. (Boehmer et al., 2003) investigated the neutron and gamma fluences and the radiation damage of the pressure vessels of WWER[1]-1000, German 1300 MW PWR[2] and 900 MW BWR[3]. They used EGS4 Monte Carlo code to calculate dpa produced by gamma particles. DART code was instead used to calculate dpa for four different nuclear reactors, namely ITER[4], HFIR[5], PWR and IFMIF[6] (Luneville et al., 2017). In addition, the effects of neutron spectrum on the calculation of dpa were evaluated in that study. A comprehensive multiscale simulation of neutron-induced damage was carried out by Choi et al. (Choi and Joo, 2013). The multiscale system consisted of a Monte Carlo Neutron transport code (MCNP), a recoil spectrum generation code (RASG (Choi and Joo, 2012)), a molecular dynamics code (LAMMPS (Plimpton, 1995)), a high-energy cascade breakup model and a simple formula to predict the amount of shear stress. Interaction of neutron and proton radiations with metal was discussed with respect to displacement damage production by Vladimirov et al. (Vladimirov and Bouffard, 2008). Lengar et al. (Lengar et al., 2016) adopted FISPACT II code (Sublet et al., 2017) and MCNP6 to evaluate the radiation damage and nuclear heating in the selected functional materials to be irradiated at JET (Joint European Torus) during deuterium-tritium plasma operation. Adrych-Brunning et al. (Adrych-Brunning et al., 2018) simulated the effect of primary interaction on damage in Zr alloys by using SPECTRA-PKA and showed that different primary interaction of neutrons and protons can produce different damage rates. Monte Carlo calculations were also used to evaluate the displacements per atom (using available codes like MCNP/X or developing his own Monte Carlo code) following NRT-dpa or other dpa calculation equations (Bess et al., 2019, 2018; Gámez et al., 2007; Kumar et al., 2012; Read and De Oliveira, 2011).

As zirconium and its alloys play an important role as fuel clad in NPPs, some papers have also focused on their radiation damage under the bombardment of neutrons or other particles. Adrych-Brunning et al. studied the effect of presence and distribution of elements in zirconium alloys on radiation damage by using SPECTRA-PKA and SRIM code (Adrych-Brunning et al., 2018) by considering both neutron and proton irradiations. In another investigation, MCNPX and SPECTER codes were used to calculate the radiation damage in Zircaloy and some micromechanical models and experimental data employed to connect the changes in electrical conductivity to radiation time (Noorikalkhoran et al., 2017). Kammenzind et al. (Kammenzind et al., 2016) studied experimentally the effect of neutron radiation on the corrosion of Zircaloy-4 in PWR primary systems. A

[1] Water-Water Energetic Reactor, comes from Russian word “VVER”(Vodo-Vodyanoi Energetichesky Reaktor)
[2] Pressurized Water Reactor
[3] Boiling Water Reactor
[4] International Thermonuclear Experimental Reactor
[5] High Flux Isotope Reactor
[6] International Fusion Materials Irradiation Facility

comprehensive review was conducted by Yan et al. (Yan et al., 2015) about the effects of ion radiation on microstructural and properties changes in Zirconium alloys. Another review focused on radiation-induced dislocation and growth in zirconium alloys (CHOI and KIM, 2013). One of the earliest studies in this field was conducted by Riley et al. (Riley and Grundy, 1972) in 1972 in which the microstructural changes in Zirconium and Zircaloy-2 under neutron bombardment were revealed by observing a set of specimens with electron microscopy.

In recent years, to increase the power generation of NPPs as an answer to developing worldwide energy demand, average burn-up of fuels has almost doubled. This increase in burn-up put the fuel clads in more stress in comparison with early NPPs (IAEA, 1993). Fuel failures in NPPs are not due to the failure of the fissile material, but of the cladding that encapsulates the fuel and separates it from the reactor coolant. Fuel failures, while not significant to plant safety, negatively affect the economics of nuclear plant operation, often requiring plant power restrictions or plant shutdown to replace the leaking assembly or, in the case of a nuclear accidents, they can lead to release of radioactive material to coolant and subsequently environment (Allen et al., 2010). As the Hot Fuel Assembly (HFA) generates the maximum portion of power in a nuclear reactor core compared with other assemblies, the maximum amount of thermal stress will occur on the fuels in this bundle, thus increasing the risk of safety issues.

In this study, radiation damage of the fuel clad in HFA is evaluated in a typical WWER-1000 reactor core. To achieve this goal, different nuclear and radiation damage codes and methods are coupled together to calculate dpa and results are compared to each other and to the experimental ones. The starting point is a full core simulation carried out by using MCNPX v2.7 code to locate the HFA and extract the exact neutron-energy spectrum. Then, PKA calculations are conducted by using, on the one hand, SPECTER and SPECTRA-PKA codes for which the location of PKAs in the sample are not known; on the other, PTRAC card of MCNPX that generates the PKAs also as a function of the position within the cell. A MATLAB kernel is developed for the preparation of SRIM code input from results of the previous codes adopted and PTRAC card. SRIM 2013 is finally used to calculate the damage parameters and simulate the visual map of damage in the sample. Effects of elemental PKAs are shown by using SPECTRA-PKA code to identify the contribution of each component on dpa. As dpa is calculated by using either NRT and arc-dpa methods or SRIM - that performs full cascade calculations based on PKA, Secondary knock-on Atoms and all their cascades- the fraction of projectile and subsequent cascades on radiation damage can be predicted as well as the effect of thermal recombination on number of dpa. Difference in dpa resulted from the analyses performed by using SPECTRA-PKA+SRIM and

MCNPX(PTRAC)+SRIM shows the importance of coordinate-dependent PKAs in estimating the radiation damage distribution.

2. Simulations

2.1. Simulation of the reactor core

The WWER-1000/V446 reactor core has a hexagonal configuration and 1/6 symmetric shape. It consists of 163 hexagonal fuel assemblies of the same geometry and produces 3000 MWth at full power. Moreover, each fuel assembly contains 311 fuel rods and 18 guiding channels for control rods or burnable poisons (AEOI, 2007). Figure 1 and 2 show the cell layout of the reactor core and structure of the pressure vessel for WWER-1000/V446 NPP, respectively. MCNPX v2.7 (ENDF/B-VII.1[1]) code (Pelowitz, 2011) is used for the full neutronic simulation of the core and pressure vessel in the Beginning Of Cycle (BOC). In this analysis, pressure vessel, fuel assemblies, fuel rods, control rods, guiding channels and other details of reactor core are considered. Side and top view input data for the MCNPX simulation are visualized in Figure 3 and 4, respectively.

MCNPX Tmesh card (mesh tally) is used to extract the power in 163 fuel assembly (tally F7) and Radial Power Peaking Factors (RPPFs) are calculated by using the following equations:

$$P_{avg} = \frac{\sum P_i}{N}, \qquad (1)$$

$$RPPF = \frac{P_i}{P_{avg}}, \qquad (2)$$

where N is the total number of fuel assemblies, P_i is the power of the i^{th} fuel assembly, and P_{avg} is their average power. To locate the HFA and validate the simulation, in Figure 5 the obtained RPPFs are compared to those reported in the FSAR[2] (AEOI, 2007) for 1/6 of the reactor core; the third entry reported in each fuel assembly is the relative error.

The simulation and FSAR data are in good agreement. The maximum RPPF, whose value is 1.29, takes place in the red-coloured fuel assembly, with a relative error of 0.31%. The proximity of the two data confirms the accuracy of the simulation approach.

Figure 6 shows the fuel structure (parts a and c) and temperature profile of fuel clad (part b) for core average and HFA (fuel clad temperature is averaged over 311 fuel rod of HFA) as calculated by Noori-Kalkhoran et al. (Noori-Kalkhoran et al., 2014). The outcome is that there is a maximum difference of about 14 °C between the two temperatures (occurring at approximately a height of 2.5

[1] Code library version
[2] Final Safety Analysis Report

m), a value that can increase in the case of an accident and can show the importance of analysing HFA from the point of view of radiation damage.

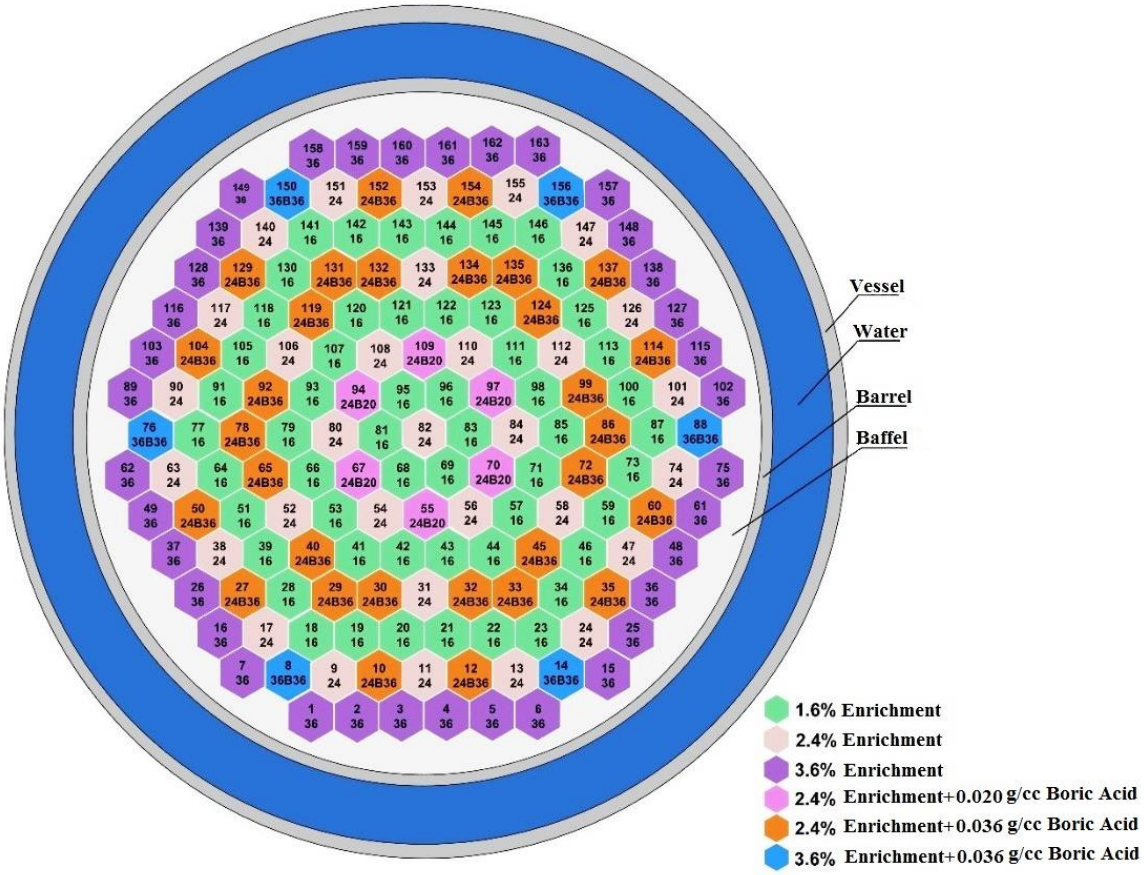

Figure 1. Schematic of the core layout of WWER-1000/V446.

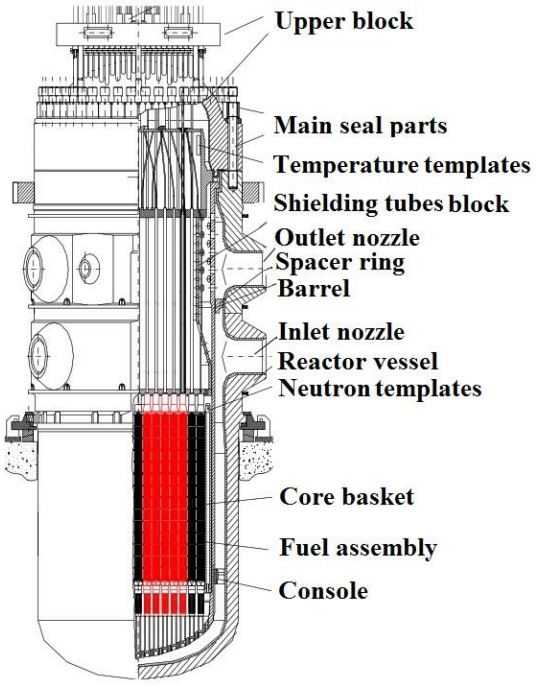

Figure 2. Schematic of core component structures and pressure vessel of WWER-1000/V446.

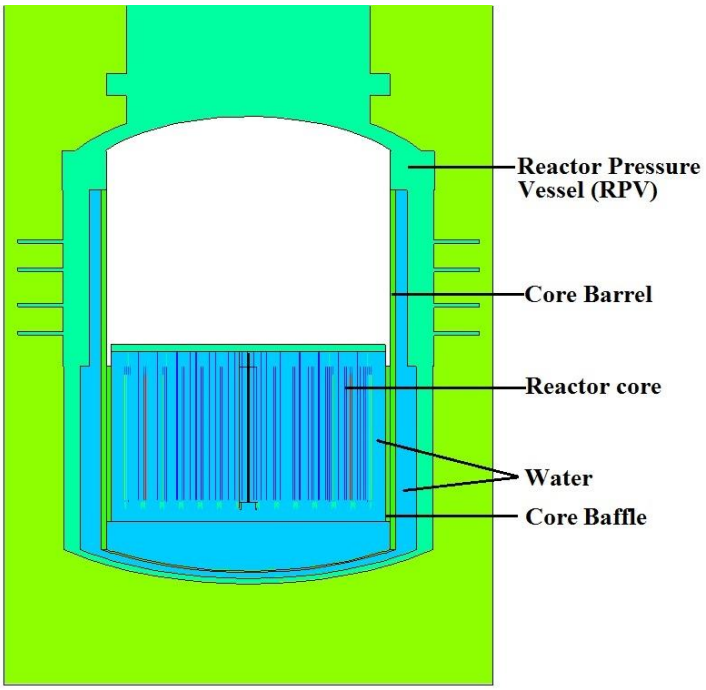

Figure 3. Side view of simulation input of MCNPX v2.7 taken by Visual Editor Ver. 24E. This figure shows the way that core component structures and pressure vessels (shown in figure 2) were simulated in MCNPX code.

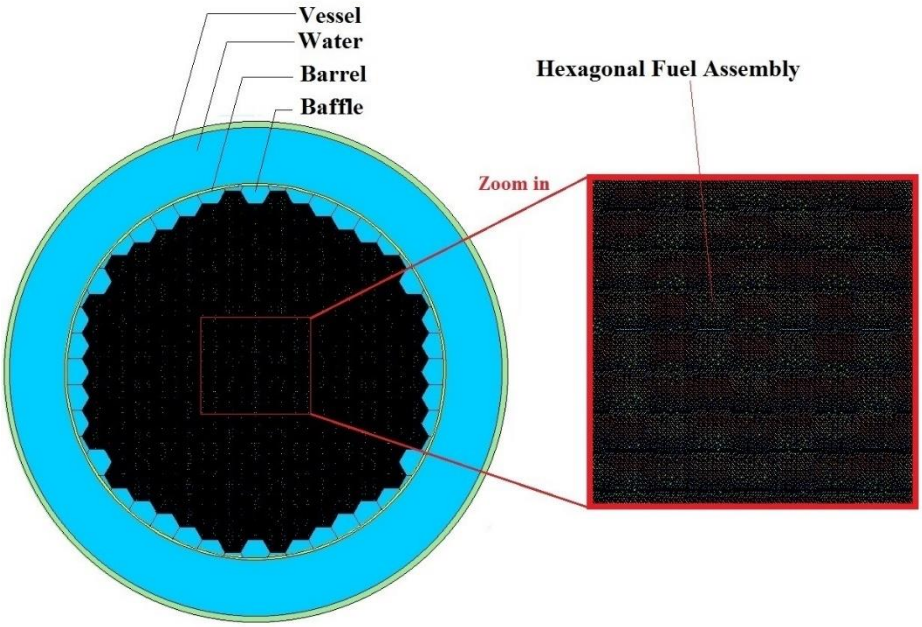

Figure 4. Top view of core simulation input of MCNPX v2.7 taken by Visual Editor ver. 24E. This figure shows the way that reactor core (shown in figure 1) was simulated in MCNPX code.

Forty-seven groups neutron-energy spectra are extracted for three different core locations (core volume-averaged, inner barrel and HFA) from MCNPX output and presented in Figure 7. For the first two, FSAR data are also available so that a comparison between them, that is in general good,

can be made. The comparison shows good agreement, confirming that neutron-energy spectra are reliable input for the estimation of radiation damage.

The spectrum of HFA (shown with a red-dashed line in Figure 7) is the average of 311 values obtained, in turn, by averaging the spectrum over each clad surface. It is clear that the flux intensity for HFA is slightly greater than that of the core average and the reason is to be found in the design of core layout. The HFA spectrum is assumed as the neutron-energy spectrum for the next step of radiation damage simulation.

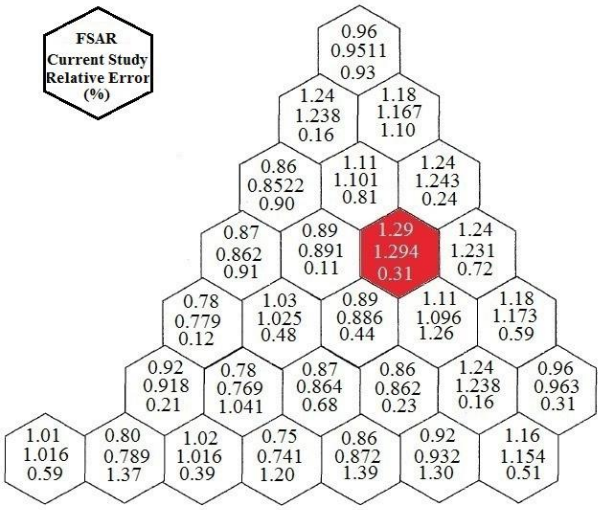

Figure 5. *RPPF* of fuel assemblies for a symmetry sector of 60 degrees, BOC and without poisoning. Comparison between FSAR and results of the current study. The red-coloured Fuel Assembly has the maximum *RPPF* whose value is 1.29.

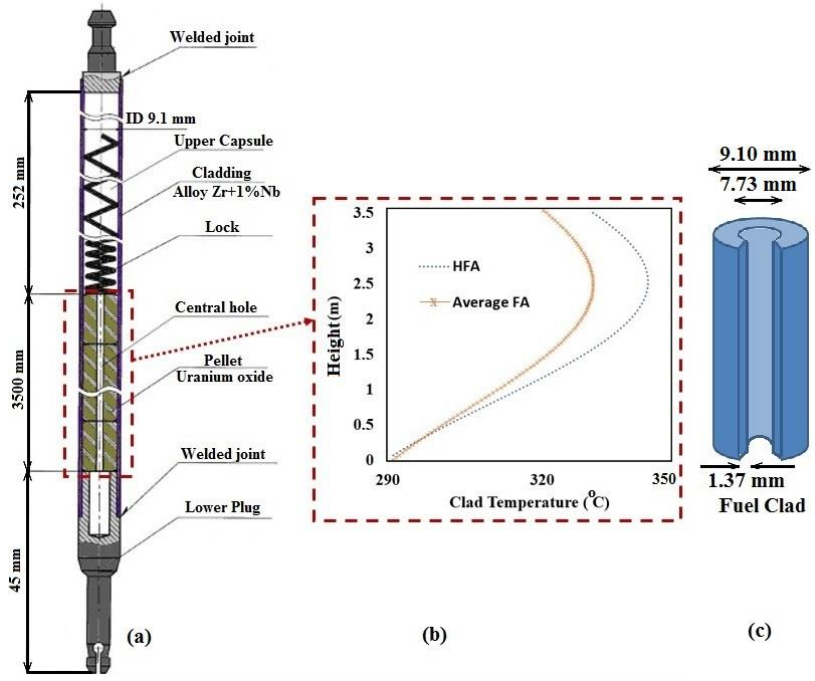

Figure 6. Fuel rod structure and profile of fuel clad temperature: (a) fuel rod structure, (b) clad temperature profiles, (c) fuel clad dimensions. A maximum difference of about 14 °C between average FA clad temperature and HFA average clad temperature occurs at a height of approximately 2.5 m.

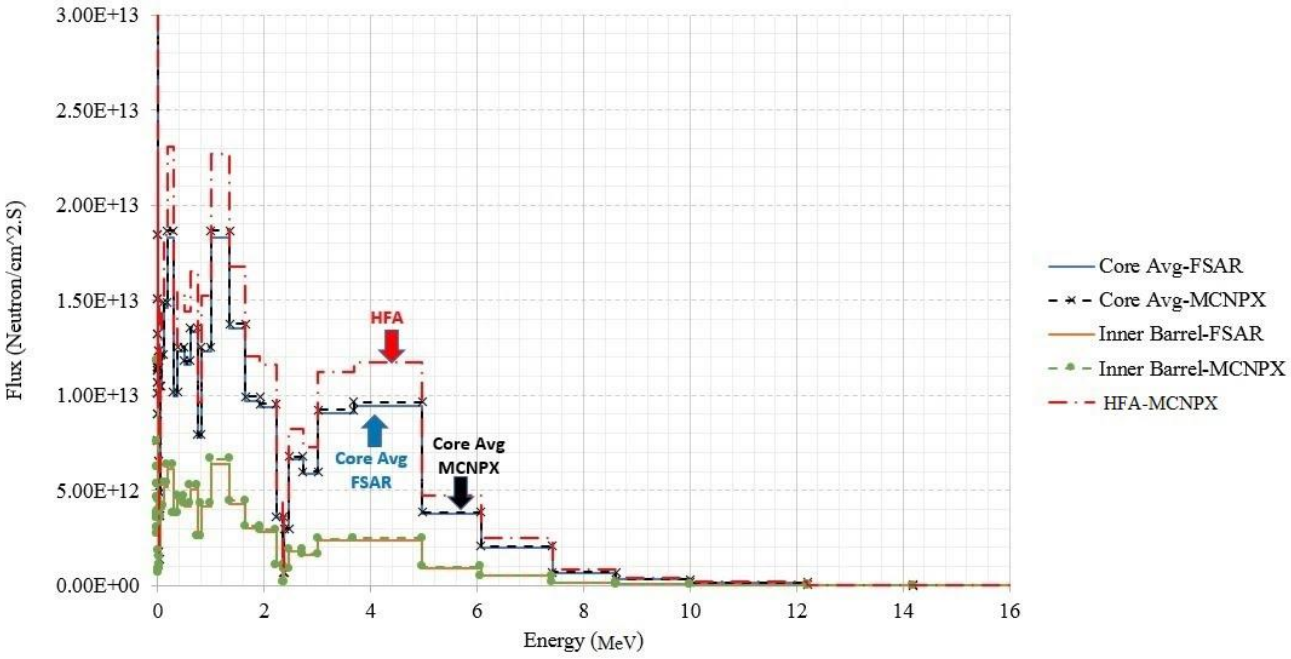

Figure 7. Neutron-energy spectrum for core volume-averaged, inner barrel and HFA. HFA neutron-energy spectrum is used as the main input for radiation damage simulation.

2.2. WWER-1000 fuel clad

The zirconium-based alloys used for nuclear fuel cladding were first developed in the US nuclear navy program in 1950s. Zirconium alloys are very common as cladding of fuel rods as they possess very low absorption cross-section of thermal neutrons. It was recognized that the corrosion performance of zirconium alloys worsened as the alloy becomes purer, with the purest metal exhibiting breakaway corrosion (Motta et al., 2015). The fuel clad of the WWER-type reactor is composed of E-110 alloy (99%Zr+1%Nb) and has been successfully employed in WWER and RBMK reactors since 1960 (Shebaldov et al., n.d.). The chemical composition and thermophysical properties of the alloy are listed in Table 1 and 2, respectively.

2.3. Primary Knock-on Atom spectrum

The probability of displacing atoms from their lattice site (σ_D) depends on the incident neutron energy and cross section, primary recoil atom energy distribution and secondary recoil atom probability (Greenwood and Smither, 1985). Mathematically, this is expressed as

$$\sigma_D(E) = \sum_i \sigma_i(E) \int_{T1}^{T2} K_i(E,T)\nu(T)dT, \qquad (3)$$

where E is the incident neutron energy, T is the recoil nucleus energy, $\sigma_i(E)$ is the nuclear cross section for channel i at energy E, $K_i(E,T)$ is neutron-atom energy transfer kernel for channel i and $\nu(T)$ is the secondary displacement function. The kernel K is simply the probability that a neutron of energy E will produce a recoil atom energy T known as Primary Knock-on Atom (PKA).

Table 1. The chemical composition of fuel rod cladding material (E-110)

Designation of element	Mass Fraction, % (not more)	Designation of element	Mass Fraction, % (not more)	Designation of element	Mass Fraction, % (not more)
Nb	0.9-1.1	H	0.0015	Sn	0.05
Fe	0.05	B	0.00005	Be	0.003
Ni	0.02	Ca	0.03	K	0.004
Al	0.008	Cd	0.00003	Li	0.0002
Ti	0.005	Cr	0.02	Mo	0.005
Si	0.02	Cu	0.005	Cl	0.003
C	0.02	Mn	0.002	F	0.003
N	0.006	Pb	0.005	Zr	98.5-99
O	0.099	Hf	0.05		

Table 2. Thermophysical properties of E-110 fuel clad alloy

Property	Temperature, °C		
	20	300	400
Thermal conductivity, W/(m.K)	17.2	20.1	20.5
Heat capacity, kJ/(kg.K)	-	0.322	0.343
Coefficient of thermal expansion,$10^{-6}K^{-1}$	5.8	6.2	6.3
Young's modulus, 10^4 MPa	9.47	7.54	7.20
Poisson's ratio	0.41	0.40	0.40
Density, 10^3 kg/m^3	6.55	6.55	6.55

As mentioned before, a two-step calculation is needed to evaluate the radiation damage in the material in terms of dpa. The first one consists in the evaluation of the spectrum of Primary Knock-on Atoms (PKAs) under a specified neutron flux; in the second step, the number of defects occurring in the lattice due to these energetic atoms is computed. SPECTER (Greenwood and Smither, 1985), SPECTRA-PKA (Gilbert et al., 2015) and PTRAC card of MCNPX are used to calculate the PKA spectrum in this article. SPECTER (ENDF/B-V[1]) computer code was written to facilitate damage calculation for any specified neutron irradiation. It adopts ENDF/B-V library (released in 1978) for nuclear reaction data and unfortunately no option to import new data libraries is available. The SPECTER computer code returns only values of PKA and dpa for pure elements (41 elements). For compound materials consisting of at most 5 elements, the SPECOMP code can

[1] Code library version

be employed to calculate dpa cross sections and import them to the SPECTER library. In this study, E-110 alloy (99%Zr+1%Nb) cross sections are built and the pertinent data (compound.out file) are added to the SPECTER library to enable SPECTER to deal with this compound material.

SPECTRA-PKA (TENDL-2017[1]) was recently developed as a module of FISPACT-II code to produce PKA spectra for any material composition. Differently from SPECTER, this code can handle modern nuclear data and complex material composition. Moreover, the new code can allow both recoil matrices and neutron spectra in any user-defined energy group structure (Gilbert et al., 2015). The available source code of SPECTRA-PKA is compiled in Linux environment to produce the executive file to be used in running the required simulations. Table 3 shows the input data for calculation of PKA spectrum by SPECOMP+SPECTER and SPECTRA-PKA (ASTM International, 1996).

Table 3. Input data for SPECOMP+SPECTER and SPECTRA-PKA

Element	Atomic number	Standard Atomic Weight (Meija et al., 2016)	Fraction (%)	Threshold energy (eV) (ASTM, 2017)	TGAM* (eV) (Greenwood and Smither, 1985)
Zr	40	91.224	99	40	142
Nb	41	92.906	1	60	111

*Effective gamma damage energy

As a third tool, PTRAC (Particle Track output) card of MCNPX is used to generate the PKAs data. PTRAC card can generate an output file that contains the history of events of all particles. In our set of simulations, to track the particle inside the fuel clad, all neutron events (TYPE=n) are considered in the specified cell (CELL=10, cell 10 determines a cell with the dimension of clad fuel element – 1.37×1.37×1.37 mm^3). The output PTRAC file[2] is processed by a kernel written in MATLAB and prepared for using as SRIM input for dpa calculations. The algorithm of simulation is shown in Figure 8.

2.4. MATLAB kernel 'PTRIM'

The kernel programmed in MATLAB is hereafter named as 'PTRIM'. PTRIM processes the PTRAC file of MCNPX, SPECTER and SPECTER-PKA outputs and prepares the SRIM (TRIM module) input file. The main tasks carried out by PTRIM are:

[1] Code library version
[2] PTRAC file is written in ASCII format.

1- PTRAC ASCII file is read by PTRIM and a new file in the TRIM input format is generated. To achieve this goal, PTRIM detects the various event IDs (5 event types: SRC, BNK, SUR, COL and TER) and end of history. Interaction events are then categorized and

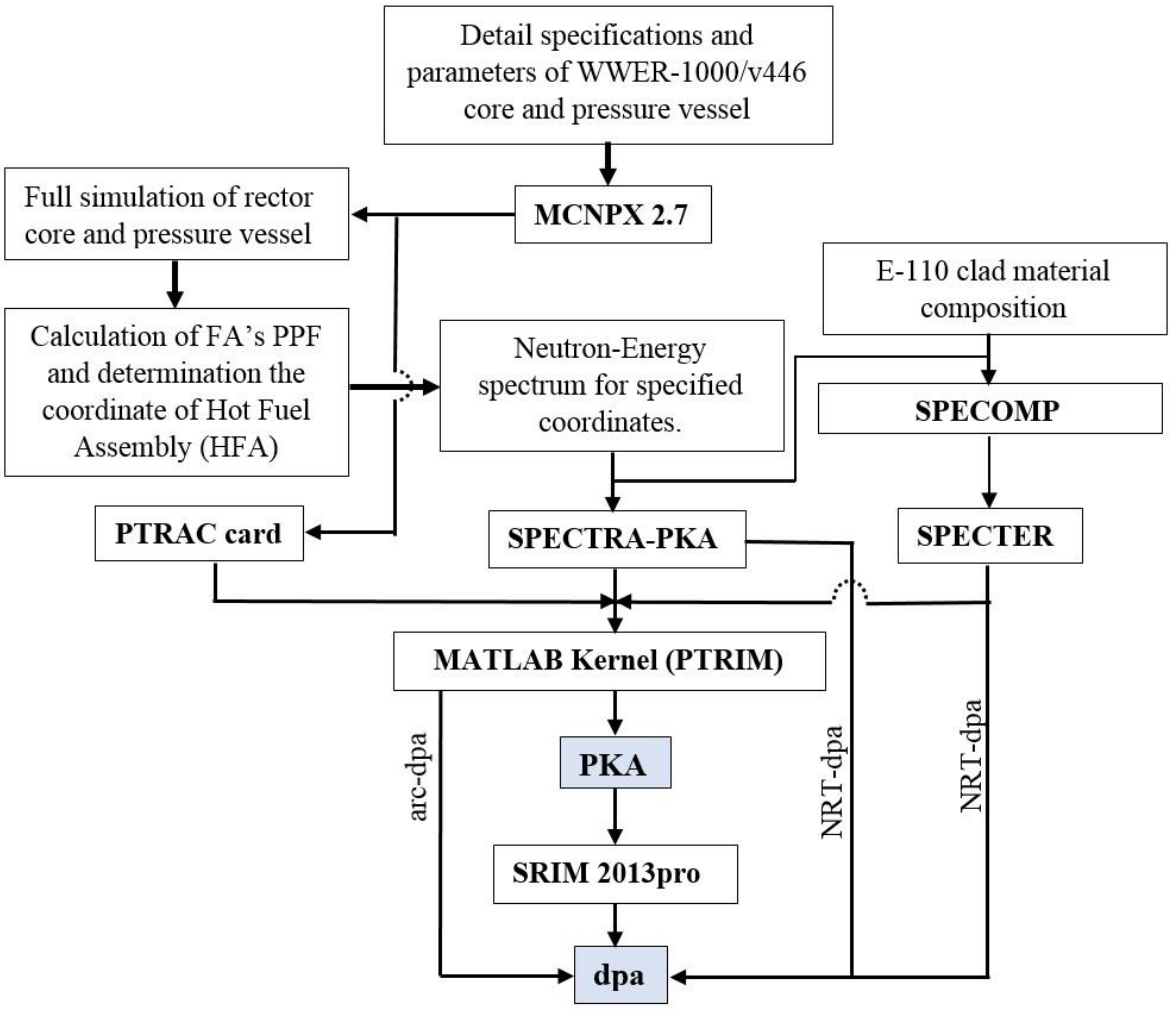

Figure 8. Algorithm of radiation damage simulation that can be split into three main steps: 1) calculation of neutron-energy spectrum, 2) calculation of PKA spectra and 3) calculation of dpa.

atomic number, coordinates (x, y, z), unit vectors singling out the direction after event (u, v, w), energy of the projectile (a neutron in this case) before and after events and the incident particle are saved to a data library. PKA spectrum is calculated according to the kinematic of interaction for elastic and inelastic collisions by using the saved library (Foderaro, 1971; *MCNP Developer's Guide Vol III*, n.d.; Stankovic et al., 2015).

2- PKA spectrum (group-averaged) is calculated from the results of step no. 1.

3- SPECTER and SPECTRA-PKA output files are read and the SRIM input file is prepared according to their generated PKA spectra. Total PKA spectrum or elemental average ones (in the case of SPECTRA-PKA) can be selected in this step. Number of PKAs can be selected by user and kernel generates the SRIM input file by considering the PKAs spectrum

on the selected number. It should be recalled that in this step, coordinates of PKAs are not considered in the generated SRIM input file (unlike the PTRAC file) as all PKAs start their tracking from point (0,0,0).

4- Calculation of dpa according to MCNPX tally's results (Bess et al., 2018) and arc-dpa equations (equations are presented in section 2.5).

2.5. Calculation of dpa and visualization of damage

SPECTER, SPECTRA-PKA, MCNPX+arc-dpa and SRIM codes are also used to simulate the radiation damage by calculating dpa. The first two codes adopt NRT method, the third one uses arc-dpa equations and the fourth one uses Binary Collision Approximation (BCA).

One of the earlier estimation of primary radiation damage was presented by Norgett, Torrens and Robinson (NRT-dpa) (Norgett et al., 1975) in 1975 where the number of Frenkel pairs formed for a given energy transfer to primary knock-on atoms was computed. Their approach is based on the Kinchin-Pease (Kinchin and Pease, 1955) model.

In dense metals, where athermal recombination of damage within energetic displacement cascades reduces the residual damage levels from the NRT calculation (recombination effect), it is advised to use "athermal recombination-corrected dpa (arc-dpa)" (Konobeev and Fischer, 2015; Konobeyev et al., 2017a; Nordlund et al., 2015),this function is presented as:

$$N_{d,arcdpa}(E) = \begin{bmatrix} 0 & when & E < E_d \\ 1 & when & E_d < E < \frac{2E_d}{0.8} \\ \frac{0.8E}{2E_d}\zeta(E) & when & \frac{2E_d}{0.8} < E < \infty \end{bmatrix}, \qquad (4)$$

which differs from the NRT-dpa for the efficiency function $\zeta(E)$ which is given by (for NRT equation $\zeta(E) = 1$):

$$\zeta(E) = \frac{1 - c_{arcdpa}}{(\frac{2E_d}{0.8})^{b_{arcdpa}}} E^{b_{arcdpa}} + c_{arcdpa}, \qquad (5)$$

In eq. (5), E is damage energy, E_d is average threshold displacement energy, b_{arcdpa} and c_{arcdpa} are unitless fitted parameters with a physical meaning. In this study, values of b_{arcdpa} and c_{arcdpa} are considered as -0.8 and 0.7, respectively (Broeders and Konobeyev, 2004; Konobeyev et al., 2017a, 2017b).

SRIM is a collection of software packages which are able to calculate many features of the transport of ions in matters (Ziegler, 2004). One of the modules of SRIM software is called TRIM, a Monte

Carlo computer program that calculates the interaction of the energetic ion with the amorphous target. TRIM accepts complex targets made of compound materials with up to eight layers, each of different materials. It provides the final 3D distribution within the studied cell of both ions and the kinetic parameters associated with the ion's energy loss. After having calculated PKAs, dpa is computed by using SPECTER, SPECTRA-PKA (NRT-dpa model), MCNPX+arc-dpa and SRIM-2013 pro (BCA) (using TRIM module).

3. Results and Discussion

Neutron-energy spectrum of averaged fuel clad in HFA (mentioned in Figure 7) is used as input for SPECTER and SPECTRA-PKA with fluence of $5.791 \cdot 10^{14}$ Neutron/cm^2. MCNPX's PTRAC file is also generated by setting the maximum number of events to write (MAX=10^7). This file is processed with the MATLAB kernel (PTRIM) to prepare both the PKA spectrum and the TRIM input file (24985 collision events are processed with PTRIM). Data of the normalized PKA spectra are shown in Figure 9 for SPECTRA-PKA and MCNPX (565 energy groups) in the top plot and SPECTER (98 energy groups) in the bottom one. All the three trends are very similar and results of MCNPX(PTRIM) (dashed line) are in good agreement with those obtained by SPECTRA-PKA (it should be considered that MCNPX uses a continuous energy cross section). SPECTER and SPECTRA-PKA adopt the same method for the computation of PKA, but with a different version of ENDF libraries, while MCNPX (PTRIM process on PTRAC file) models neutron collisions though a Monte Carlo method (that is a probabilistic one).

Figure 10 shows the elemental PKAs (a) and their contributions to dpa (b) resulted from SPECTRA-PKA. According to the data reported in this figure, Zr, Nb and total PKA spectra have very similar trends. This is due do the fact that atomic and mass numbers of Zr and Nb are very close (and, in turn, close to the mass number of Zircaloy) and so the behaviour of projectile interaction with these atoms is almost the same. Values of zirconium PKA are approximately 10^3 times greater than those of Nb and as the mass fraction of Zr is approximately 99%, the calculated contribution to dpa of this element is 99.246% of the total. That of Nb amounts to 0.731% whereas the remaining fraction (0.023%) is provided by other materials that are produced from different interaction of neutrons with the sample. In particular, these are H, He, Kr, Rb, Sr and Y whose contributions correspond to $8.26 \cdot 10^{-5}$ %, $3.80 \cdot 10^{-4}$ %, $9.05 \cdot 10^{-17}$ %, $1.51 \cdot 10^{-10}$ %, $1.06 \cdot 10^{-2}$ % and $1.21 \cdot 10^{-4}$ %, respectively.

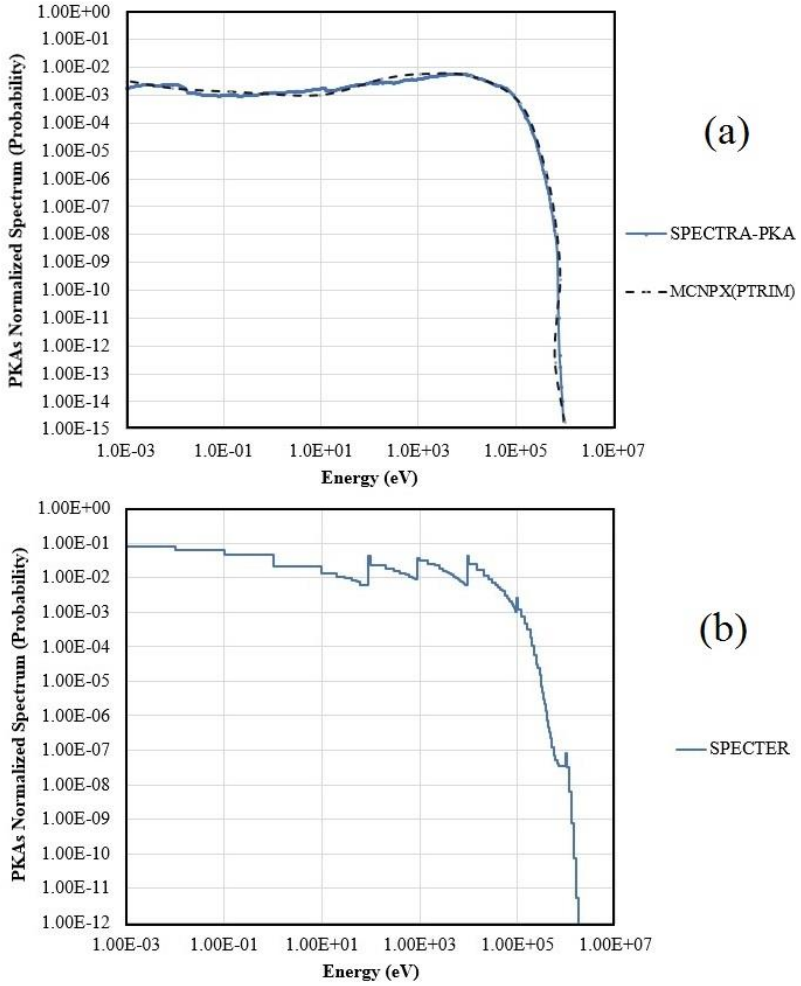

Figure 9. PKA spectra calculated by (a) MCNPX(PTRIM) (ENDF/B-VII.1) and SPECTRA-PKA (TENDL-2017) for 565 energy groups and (b) SPECTER (ENDF/B-V) codes for 98 energy groups.

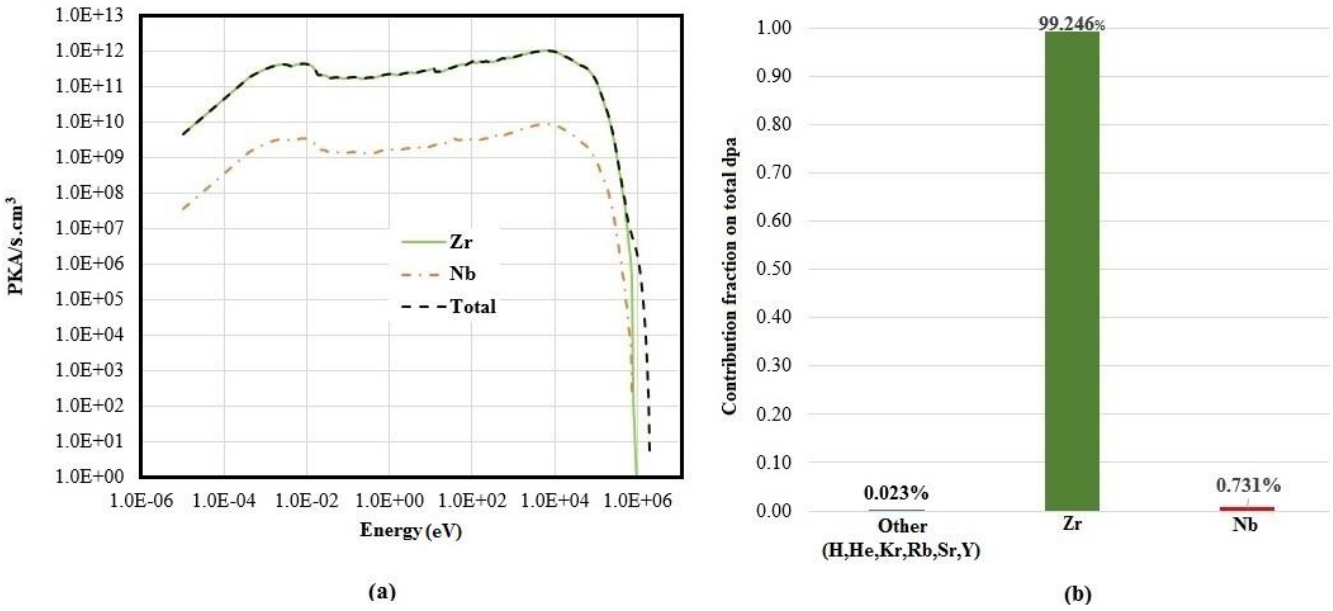

Figure 10. (a) Elemental PKA spectra and (b) their contribution to dpa.

SRIM2013pro is used to calculate the dpa and visualize damage events. TRIM input is prepared by MATLAB kernel (PTRIM). Table 4 shows the input parameters for SRIM (TRIM module). In this table, displacement energy is the energy that a recoil needs to overcome the lattice forces, surface binding energy is the energy that relates to the target atoms that leave the target surface and lattice binding is the energy that every recoiling target atom loses when it is about to leave the lattice site. To increase the computational speed of TRIM module, the user can select different methods to estimate the damage based on details of the collision kinetics. "Full Damage Cascade" (F-C) includes all normal kinetics of ion penetrating the target. It considers all the generation of knock-on atoms whose energy are above the threshold energy of lattice atoms so it includes the secondary knock-on atoms and other generation cascades. The "Quick" calculation (that is also named "K-P" as it uses Kinchin and Pease theory (Kinchin and Pease, 1955)) omits target atom cascades and limits the calculation to the ion trajectories. It should be considered that the outcome of TRIM suffers two major limitations: a) build-up of ions or damages are disregarded (it means that TRIM tracks each ion in a bare material without considering the damage generated from the previous ones); b) temperature is set as 0 K, meaning that there are no thermal effects that either change the distribution of ions (thermal diffusion) or affect the target damage (thermal annealing) (Ziegler, 2004). Both these limitations can lead to errors in the outcome of the computation. Applying modified equations for dpa calculation like arc-dpa (that considers thermal recombination) on SRIM calculations can somewhat compensate the latter limitation (Nordlund et al., 2015). Table 5 shows the outcome of SRIM calculations for TRIM input file generated from PTRAC file of MCNPX and SPECTRA-PKA output file. In both cases, the MATLAB kernel PTRIM is used for the preparation of TRIM input file. It should be noted that 10^6 particles are considered for SPECTRA-PKA file and PTRAC file is generated with MAX=10^7 (the maximum number of events per history to write in PTRAC file). Calculations are performed for both full-cascade and K-P methods. Values of dpa reported in the last column of this table are calculated by considering the "total displacement" listed in the second column. As shown in the table, values of total displacements for F-C calculations are almost as twice as those for the K-P method for both PTRAC+SRIM and SPECTRA-PKA+SRIM codes. This discrepancy is the result of differences in the collision kinetics: K-P only tracks the primary ion trajectories whereas in the F-C method target atom cascades are also allowed. Therefore, it can be concluded that projectile ions and target cascade atoms generated from PKA provide a similar contribution to radiation damage (approximately 50% each). Despite having similar PKA spectra, values of displacements from SPECTRA-PKA+SRIM calculations are greater than those attained from PTRAC+SRIM. One of the reasons of this phenomenon can be the feature of using coordinate dependent PKA as input of the latter code. Indeed, the input file of TRIM

generated from PTRAC is a function of the location whereas for SPECTRA-PKA all the PKAs will start form the origin of the coordinate system. The ion range in the sample is also listed in the same table for average, lateral and radial directions.

Table 4. Input parameters for SRIM calculation

Element	Atomic number	Weight (amu)	Fraction (%)	Displacement energy (eV)	Lattice binding energy (eV)	Surface binding energy (eV)
Zr	40	91.22	99	40	3	6.33
Nb	41	92.90	1	60	3	7.59

Table 5. SRIM calculation results

Method of calculation	Total displacement /neutron	Total vacancy/neutron	Replacement collisions/neutron	Ion Range (A) Average	Lateral	Radial	dpa/s
PTRAC+SRIM (K-P)	15	15	0	-	-	-	2.022E-07
SPECTRA-PKA +SRIM (K-P)	20	20	0	-	-	-	2.695E-07
PTRAC+SRIM (F-C)	27	25	2	803.2E+04	408.3E+03	632.5E+03	3.639E-07
SPECTRA-PKA +SRIM (F-C)	38	35	3	-	-	-	5.121E-07

Table 6 lists values of dpa calculated by SPECTER, SPECTRA-PKA, MCNPX+arc-dpa and by coupling separately SRIM-2013pro with PTRAC and SPECTRA-PKA. In the same table the results are compared to experimental values. As it is evident from the table, data obtained from MCNPX+arc-dpa are close to experimental results as thermal recombination effect is considered in arc-dpa methodology (eqs 4 and 5) through function $\zeta(E)$ and fitted parameters b and c in eq. (5). Other simulation methods predict values of dpa 2-4 times higher than the experimental ones as effects of thermal damage recombination are disregarded. NRT method predicts an amount of dpa/s lower than that attained with BCA. More in detail, values of dpa/s calculated by BCA (K-P) method are closer to NRT ones in comparison with F-C calculations as in the former approach only PKAs are tracked while in the latter atom cascades are also tracked.

Table 6. Comparison between values of displacement per atom (dpa)

Parameter	SPECTER (ENDF/B-V)	SPECTRA-PKA (TENDL-2017)	MCNPX +arc-dpa (ENDF/B-VII.1)	PTRAC+SRIM (K-P)	SPECTRA-PKA+SRIM (K-P)	PTRAC+SRIM (F-C)	SPECTRA-PKA+SRIM (F-C)	Experimental values* (dpa/s)
Average PKA energy (eV)	5.517E+03	6.069E+03	-	5.741E+03	-	-	-	**0.6-1.1E-7** (PWR)**
dpa/s	1.865E-07 (NRT)	1.845E-07 (NRT)	0.632E-07 (arc-dpa)	2.022E-07	2.695E-07	3.639E-07	5.121E-07	**0.6-1.3E-7** (WWER)***

*Values of dpa for Zircaloy were extracted from different references for similar PWRs and WWERs (Neutron-Energy spectrum of some PWRs are similar to that of WWERs). As these values have been measured for either different radiation locations inside the core or different experimental methods, dpa is reported in the table as a range.

**(Korea Atomic Energy Research Institute (KAERI), 2001)

***(AEOI, 2007; Perez-Feró et al., 2007)

Finally, 3D visualization of target damage and target ionization for the clad sample are presented for K-P and F-C calculations (PTRAC+SRIM) in Figures 11-14. By comparing Figures 11 and 12 and, in turn, 13 and 14, it is shown that both methods predict for target damage and ionization a very similar distribution map in which, in addition to some local maxima, the two overall maxima

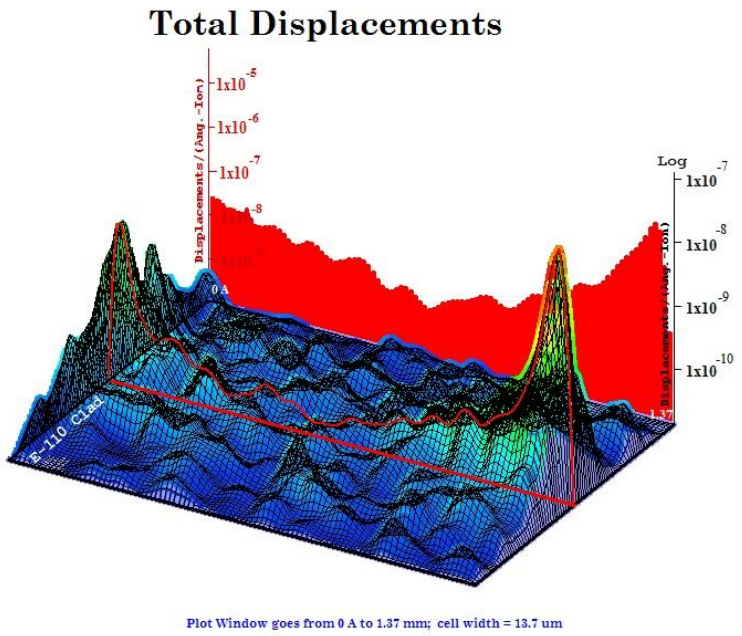

Figure 11. 3D visualization of total displacement distribution in fuel clad sample obtained by SRIM (K-P).

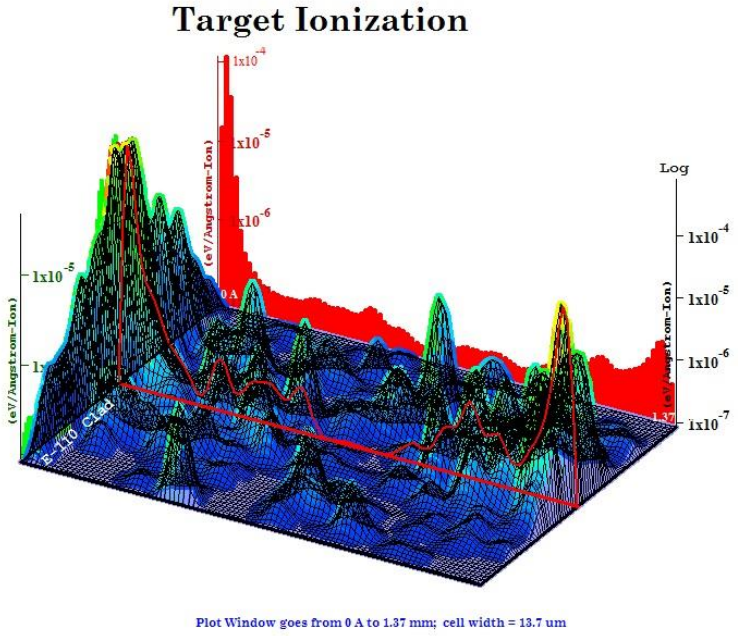

Figure 12. 3D visualization of target ionization distribution in fuel clad sample obtained by SRIM (K-P).

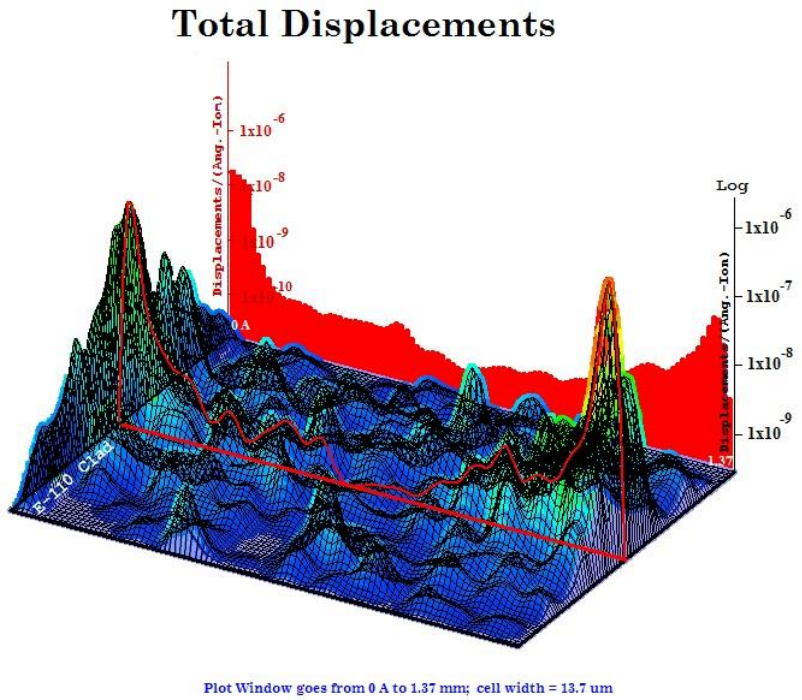

Figure 13. 3D visualization of total displacement distribution in fuel clad sample obtained by SRIM (F-C).

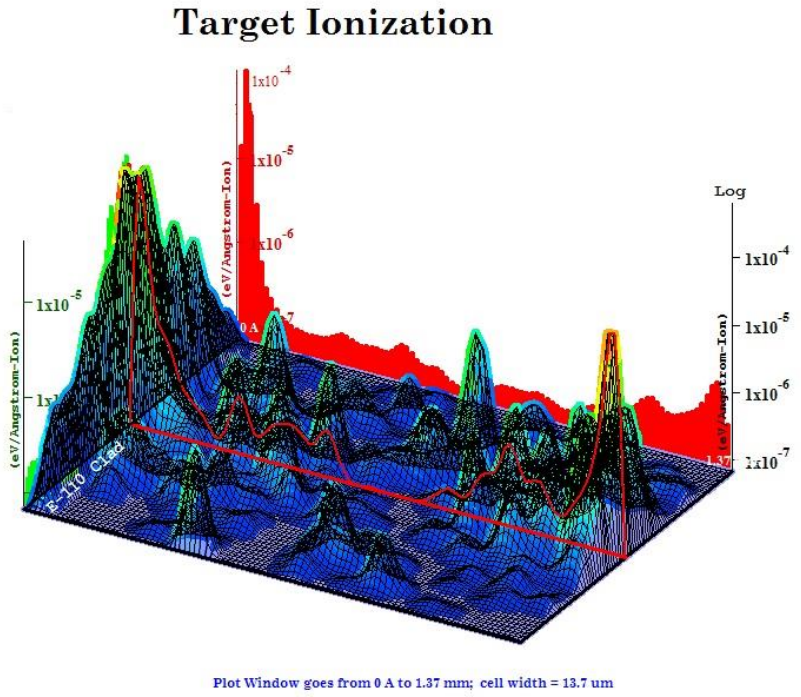

Figure 14. 3D visualization of target ionization distribution in fuel clad sample obtained by SRIM (F-C).

occur along the two sides of the clad sample. Sputtering, i.e. the removal of near-surface atoms from the target, can be one of the reasons for damage peaks to be located here; this is justified by the fact that the near-surface binding energy for the clad sample is about 7 eV (see Table 4), a threshold that can be overcome by most of the neutrons in the flux spectrum.

4. Conclusions

One of the main concerns in nuclear safety is to maintain the integrity of structural materials of nuclear power plants in case of accident to avoid the release of radioactive materials. Fuel clad is one of these materials that, in addition to its main role of assuring heat transfer from fuel to coolant, also acts as a second barrier in terms of Defense In Depth. Radiation can affect the integrity of fuel clad by displacing atoms in the material lattice on the one hand and transmuting materials to other elements on the other. In this study, neutron-induced radiation damage is investigated in Zircaloy fuel clad by calculating PKA and dpa with various codes and their coupling. SPECTER, SPECTRA-PKA and PTRAC file of MCNPX are used to obtain the PKA and, in a subsequent stage, dpa is calculated by SPECTER (NRT-dpa), SPECTRA-PKA (NRT-dpa), MCNPX+arc-dpa (arc-dpa) and the coupling of PTRAC and SPECTRA-PKA with SRIM code. The main outcomes of the paper are collected in Table 5 and 6 from which comparison of results between NRT-dpa, arc-dpa, BCA and coupling calculations of dpa can be performed, leading to the following conclusions:

- According to results, values of dpa calculated through arc-dpa equations (MCNPX+arc-dpa method) are in good agreement with experimental ones in comparison with other methods and couplings, as the former method considers the thermal recombination effects in atom lattice. arc-dpa value is almost 1/3 (~34%) of NRT-dpa calculated by SPECTER and SPECTRA-PKA as also reported in another reference (Nordlund et al., 2015).
- as expected (Nordlund et al., 2015), the F-C method implemented in SRIM predicts values of dpa that are almost as twice as those obtained from the K-P one;
- the values of dpa calculated following the NRT approach (SPECTER and SPECTRA-PKA) are different from those attained by both using BCA method (PTRAC+SRIM) and coupling of SPECTRA-PKA and SRIM codes. Among the last two, the closest result to NRT-dpa is provided by BCA (K-P) method that neglects the secondary knock-on atoms and atom cascades;
- importance of using coordinate-dependent PKA on dpa calculations is evident in the discrepancies that occur between PTRAC+SRIM and SPECTRA-PKA+SRIM output data, as the former considers the position of PKAs in the sample while the latter omits this factor;
- by using PTRAC file of MCNPX that generates coordinate-dependent PKAs followed by SRIM for dpa calculations, it is possible to visualize a meaningful neutron-induced radiation damage distribution map.
- some error sources can affect the results of dpa calculations such as: methods of calculation of different codes and their limitations and assumptions, cross-section libraries (ENDF,

TENDL, etc, more information can be found in (Griffin et al., 2016; Stoller et al., 2015)) and libraries data processing (more information can be found in SPECTER (Greenwood and Smither, 1985), SPECTRA-PKA (Gilbert et al., 2015), MCNPX (Pelowitz, 2011) and NJOY (Macfarlane and Muir, 1994) code manuals).

Calculation of dpa and PKA with different methods and couplings and comparison of their values (especially against experimental ones) can be a good index about the validity of the methods themselves and their assumptions, thus gaining an insight into their strengths and weaknesses with the goal to propose appropriate modifications. The prospective goal is to predict the effect of dpa (in addition to other radiation damage phenomena) on the macroscopic properties of structural materials in NPPs.

Acknowledgements

This research has been developed under the auspices of European Union's Horizon 2020 (EU H2020) research and innovation programme Marie Skłodowska-Curie Actions COFUND grant SIRCIW, agreement no. 663830.

References

Adrych-Brunning, A., Gilbert, M.R., Sublet, J.-C., Harte, A., Race, C.P., 2018. Modelling the interaction of primary irradiation damage and precipitates: Implications for experimental irradiation of zirconium alloys. J. Nucl. Mater. 498, 282–289. https://doi.org/10.1016/J.JNUCMAT.2017.10.022

AEOI, 2007. Bushehr Nuclear Power Plant Fainaly Safety Analysis Report.

Allen, T., Busby, J., Meyer, M., Petti, D., 2010. Materials challenges for nuclear systems. Mater. Today 13, 14–23. https://doi.org/10.1016/S1369-7021(10)70220-0

ASTM, 2017. Standard Practice for Investigating the Effects of Neutron Radiation Damage Using Charged-Particle Irradiation 96, 1–21. https://doi.org/10.1520/E0521-16.

ASTM International, 1996. ASTM E521-96 Standard Practice for Neutron Radiation Damage Simulation by Charged-Particle Irradiation. https://doi.org/https://doi.org/10.1520/E0521-96

Bess, J.D., Parry, J.R., Hill, C.M., Woolstenhulme, N.E., Jensen, C.B., McQuate, K.G., 2018. Comparison of Displacement Damage Calculations Supporting MIMIC Analysis and Design for TREAT. Trans. Am. Nucl. Soc. 119.

Bess, J.D., Woolstenhulme, N.E., Jensen, C.B., Parry, J.R., Hill, C.M., 2019. Nuclear characterization of a general-purpose instrumentation and materials testing location in TREAT. Ann. Nucl. Energy 124, 270–294. https://doi.org/10.1016/J.ANUCENE.2018.10.011

Boehmer, B., Konheiser, J., Noack, K., Rogov, A., Borodkin, G., Polke, E., Vladimirov, P., 2003. NEUTRON AND GAMMA FLUENCE AND RADIATION DAMAGE PARAMETERS OF EX-CORE COMPONENTS OF RUSSIAN AND GERMAN LIGHT WATER REACTORS, in: Reactor Dosimetry in the 21st Century. WORLD SCIENTIFIC, pp. 286–294. https://doi.org/10.1142/9789812705563_0036

Broeders, C.H.M., Konobeyev, A.Y., 2004. Defect production efficiency in metals under neutron irradiation. J. Nucl. Mater. 328, 197–214. https://doi.org/10.1016/J.JNUCMAT.2004.05.002

CHOI, S. IL, KIM, J.H., 2013. RADIATION-INDUCED DISLOCATION AND GROWTH BEHAVIOR OF ZIRCONIUM AND ZIRCONIUM ALLOYS – A REVIEW. Nucl. Eng. Technol. 45, 385–392. https://doi.org/10.5516/NET.07.2013.035

Choi, Y.H., Joo, H.G., 2013. Multiscale simulation of neutron induced damage in tritium breeding blankets with different spectral shifters. Fusion Eng. Des. 88, 2471–2475. https://doi.org/10.1016/J.FUSENGDES.2013.05.085

Choi, Y.H., Joo, H.G., 2012. Analysis of neutron spectrum effects on primary damage in tritium breeding blankets. J. Nucl. Mater. 426, 16–25. https://doi.org/10.1016/J.JNUCMAT.2012.04.002

Foderaro, A., 1971. The elements of neutron interaction theory. MIT Press.

Gámez, L., Martínez, E., Perlado, J.M., Cepas, P., Caturla, M.J., Victoria, M., Marian, J., Arévalo, C., Hernández, M., Gómez, D., 2007. Kinetic Monte Carlo modelling of neutron irradiation damage in iron. Fusion Eng. Des. 82, 2666–2670. https://doi.org/10.1016/J.FUSENGDES.2007.04.040

Gilbert, M.R., Marian, J., Sublet, J.-C., 2015. Energy spectra of primary knock-on atoms under neutron

irradiation. J. Nucl. Mater. 467, 121–134. https://doi.org/10.1016/J.JNUCMAT.2015.09.023

Greenwood, L.R., Smither, R.K., 1985. SPECTER: Neutron Damage Calculations for Materials Irradiation, ANL/FPP/TM-197.

Griffin, P.J., Sjostrand, H., Simakov, S.P., 2016. Nuclear Reaction Data and Uncertainties for Radiation Damage.

IAEA, 1993. Impact of extended burnup on the nuclear fuel cycle, Technology, IAEA-TECDOC-699

Iwamoto, Y., Niita, K., Sawai, T., Ronningen, R.M., Baumann, T., 2013. Displacement damage calculations in PHITS for copper irradiated with charged particles and neutrons. Nucl. Instruments Methods Phys. Res. Sect. B Beam Interact. with Mater. Atoms 303, 120–124. https://doi.org/10.1016/J.NIMB.2012.11.023

Kammenzind, B.F., Gruber, J.A., Bajaj, R., Smee, J.D., Head, H., Carolina, S., 2016. Neutron Irradiation Effects on the Corrosion of Zircaloy-4 in a PWR Environment 18 th International Symposium on Zirconium in the Nuclear Industry.

Kinchin, G.H., Pease, R.S., 1955. The Displacement of Atoms in Solids by Radiation. Reports Prog. Phys. 18, 301. https://doi.org/10.1088/0034-4885/18/1/301

Konobeev, A., Fischer, U., 2015. DPA and gas production in intermediate and high energy particle interactions with accelerator components, in: Proceedings of HB2014, THO4AB02.

Konobeyev, A.Y., Fischer, U., Korovin, Y.A., Simakov, S.P., 2017a. Evaluation of effective threshold displacement energies and other data required for the calculation of advanced atomic displacement cross-sections. Nucl. Energy Technol. 3, 169–175. https://doi.org/10.1016/J.NUCET.2017.08.007

Konobeyev, A.Y., Fischer, U., Pereslavtsev, P.E., Simakov, S.P., 2017b. Arc-dpa cross-sections for high priority elements, in: NEA Nuclear Data Week & JEFF Meetings. Boulogne-Billancourt, France.

Korea Atomic Energy Research Institute(KAERI), 2001. Irradiation Damage for Zirconium-based Alloys, KAERI/TR-1820/2001

Kumar, V., Raghaw, N.S., Palsania, H.S., 2012. A Monte Carlo Code for Radiation Damage by Neutrons. Nucl. Sci. Eng. 172, 151–163. https://doi.org/10.13182/NSE11-41

Lengar, I., Čufar, A., Conroy, S., Batistoni, P., Popovichev, S., Snoj, L., Syme, B., Vila, R., Stankunas, G., 2016. Radiation damage and nuclear heating studies in selected functional materials during the JET DT campaign. Fusion Eng. Des. 109–111, 1011–1015. https://doi.org/10.1016/J.FUSENGDES.2016.01.033

Lunéville, L., Simeone, D., Jouanne, C., 2006. Calculation of radiation damage induced by neutrons in compound materials. J. Nucl. Mater. 353, 89–100. https://doi.org/10.1016/J.JNUCMAT.2006.03.006

Luneville, L., Sublet, J.C., Simeone, D., 2017. Impact of nuclear transmutations on the primary damage production: The example of Ni based steels. J. Nucl. Mater. https://doi.org/10.1016/J.JNUCMAT.2017.06.039

Macfarlane, R., Muir, D.W., 1994. The NJOY Nuclear Data Processing System, Version 91, LA-12740-M

MCNP Developer's Guide Vol III, LA-CP-03-0284.

Meija, J., Coplen, T.B., Berglund, M., Brand, W.A., De Bièvre, P., Gröning, M., Holden, N.E., Irrgeher, J., Loss, R.D., Walczyk, T., Prohaska, T., 2016. Atomic weights of the elements 2013 (IUPAC Technical Report). Pure Appl. Chem. 88, 265–291. https://doi.org/10.1515/pac-2015-0305

Motta, A.T., Couet, A., Comstock, R.J., 2015. Corrosion of Zirconium Alloys Used for Nuclear Fuel Cladding. Annu. Rev. Mater. Res. 45, 311–343. https://doi.org/10.1146/annurev-matsci-070214-020951

Noori-Kalkhoran, O., Minuchehr, A., Shirani, A. saied, Rahgoshay, M., 2014. Full scope thermal-neutronic analysis of LOFA in a WWER-1000 reactor core by coupling PARCS v2.7 and COBRA-EN. Prog. Nucl. Energy 74, 193–200. https://doi.org/10.1016/J.PNUCENE.2014.03.006

Noorikalkhoran, O., Sevostianov, I., 2017. Micromechanical modeling of neutron irradiation induced changes in yield stress and electrical conductivity of zircaloy. Int. J. Eng. Sci. 120, 119–128. https://doi.org/10.1016/J.IJENGSCI.2017.07.002

Nordlund, K., Sand, A.E., Granberg, F., Zinkle, S.J., Stoller, R., Averback, R.S., Suzudo, T., Malerba, L., Banhart, F., Weber, W.J., Willaime, F., Dudarev, S., Simeone, D., 2015. Primary Radiation Damage in Materials, NEA/NSC/DOC(2015)9.

Norgett, M.J., Robinson, M.T., Torrens, I.M., 1975. A proposed method of calculating displacement dose rates. Nucl. Eng. Des. 33, 50–54. https://doi.org/10.1016/0029-5493(75)90035-7

Pelowitz, D.B., 2011. MCNPX User Manual Version 2.7.0, LA-CP-11-00438.

Perez-Feró, E., Gyori, C., Matus, L., Vasáros, L., Hózer, Z., Windberg, P., Maróti, L., Horváth, M., Nagy, I., Pintér-Csordás, A., Novotny, T., 2007. Experimental database of E110 claddings exposed to accident conditions, AEKI-FRL-2007-123-01/01.

Plimpton, S., 1995. Fast Parallel Algorithms for Short-Range Molecular Dynamics. J. Comput. Phys. 117, 1–19. https://doi.org/10.1006/JCPH.1995.1039

Read, E.A., De Oliveira, C.R.E., 2011. a Functional Method for Estimating Dpa Tallies in Monte Carlo Calculations of Light Water Reactors. Int. Conf. Math. Comput. Methods Appl. to Nucl. Sci. Eng.

Riley, A., Grundy, P.J., 1972. A study by electron microscopy of neutron damage in Zirconium and Zircaloy-2. Phys. Status Solidi 14, 239–247. https://doi.org/10.1002/pssa.2210140129

Robinson, M.T., 1994. The binary collision approximation: Background and introduction. Radiat. Eff. Defects Solids null, 3–20. https://doi.org/10.1080/10420159408219767

Shebaldov, P., Peregud, M., Nikulina, A., Bibilashvili, Y., Lositski, A., Kuz'menko, N., Belov, V., Novoselov, A., n.d. E110 Alloy Cladding Tube Properties and Their Interrelation with Alloy Structure-Phase Condition and Impurity Content, in: Zirconium in the Nuclear Industry: Twelfth International Symposium. ASTM International, 100 Barr Harbor Drive, PO Box C700, West Conshohocken, PA 19428-2959, pp. 545-545–15. https://doi.org/10.1520/STP14316S

Stankovic, J., Marinkovic, P., Ciraj-Bjelac, O., Kaljevic, J., Arandjic, D., Lazarevic, D., 2015. Toward utilization of MCNP5 particle track output file for simulation problems in photon spectrometry. Comput. Phys. Commun. 195, 77–83. https://doi.org/10.1016/J.CPC.2015.05.003

Stoller, R.E., Greenwood, L.R., Simakov, S.P., 2015. Primary Radiation Damage Cross Sections. Vienna, Austria, INDC(NDS)- 0691.

Sublet, J.-C., Eastwood, J.W., Morgan, J.G., Gilbert, M.R., Fleming, M., Arter, W., 2017. FISPACT-II: An Advanced Simulation System for Activation, Transmutation and Material Modelling. Nucl. Data Sheets 139, 77–137. https://doi.org/10.1016/J.NDS.2017.01.002

Vladimirov, P., Bouffard, S., 2008. Displacement damage and transmutations in metals under neutron and proton irradiation. Comptes Rendus Phys. 9, 303–322. https://doi.org/10.1016/J.CRHY.2008.02.004

Yan, C., Wang, R., Wang, Y., Wang, X., Bai, G., 2015. Effects of ion irradiation on microstructure and properties of zirconium alloys-A review. Nucl. Eng. Technol. 47, 323–331. https://doi.org/10.1016/j.net.2014.12.015

Ziegler, J.F., 2004. SRIM-2003. Nucl. Instruments Methods Phys. Res. Sect. B Beam Interact. with Mater. Atoms 219–220, 1027–1036. https://doi.org/10.1016/J.NIMB.2004.01.208